

## Adsorption of Pb(II) on Calix[4]arene Derivatives: Kinetics and Isotherm Studies

Busroni Busroni<sup>1\*</sup>, Dwi Siswanta<sup>2</sup>, Jumina Jumina<sup>2</sup>, Sri Juari Santosa<sup>2</sup>, and Chairil Anwar<sup>2</sup>

<sup>1</sup>Department of Chemistry, Faculty of Mathematics and Natural Sciences, Jember University, Jl. Kalimantan 37, Jember 681752, East Java, Indonesia

<sup>2</sup>Department of Chemistry, Faculty of Mathematics and Natural Sciences, Universitas Gadjah Mada, Sekip Utara, Yogyakarta 55281, Indonesia

\* **Corresponding author:**

tel: +62-81803516287

email: busroni.fmipa@unej.ac.id

Received: November 23, 2021

Accepted: September 30, 2022

DOI: 10.22146/ijc.70665

**Abstract:** This study aims to investigate the application of two calix[4]arene derivatives named 5,11,17,23-tetra-(*t*-butyl)-25,26,27,28-tetrahydroxycalix[4]arene (TBCA) and 5,11,17,23-tetra-(*t*-butyl)-26,27,28-tribenzoyloxycalix[4]arene (TBMTCA) as adsorbents of Pb(II) from aqueous solution in a batch system. Adsorption was carried out by varying pH solution, exposure time, and concentration. The kinetics was evaluated based on the adsorption in various exposure times using the Lagergren and Ho equations, while the isotherms were analyzed based on the adsorption in various Pb(II) concentrations using the Langmuir and Freundlich equations. Furthermore, the isotherm model showed the Pb(II) adsorption of TBCA and TBMTCA followed Langmuir model with a capacity of 137.29 and 128.46 mg/g, respectively. Based on the adsorption capacity, both adsorbents are the potential for the removal of heavy metal cations from polluted water.

**Keywords:** TBCA; TBMTCA; adsorption capacity; kinetic; isotherm

### ■ INTRODUCTION

Wastewater pollution originates from various industries and potentially deteriorates public health. Specifically, heavy metal pollutants are already polluting some Indonesian rivers [1]. Lead cation, (Pb(II)), one of the hazardous metals, has many applications in industrial activities, such as battery manufacturing, paint, and paper industries. The Pb(II) concentration in waters does not depend on the season but on the depth of the seas. The ions present in water can enter the body of fish and other aquatic animals. Generally, the natural Pb(II) level in water is 0.03 g/mL in seawater and 0.30 g/mL in the river. Furthermore, Pb(II) cations could react with -SH groups in proteins, enzymes, and blood to disrupt chemical reactions in the human body. They enter the body through food, drink, and skin penetration. They can also replace the position of calcium in human and animal bones. This metal potentially inhibits the activity of enzymes involved in the formation of hemoglobin, thereby causing anemia [2]. In general, Pb(II) interferes the

physiological activities of cell metabolism in plants, animals, and humans by accelerating the formation of reactive oxygen species as well as inhibiting the action of bivalent and other monovalent metals in the body. Before being released into the ecosystem, special methods are needed to reduce Pb(II) concentrations in wastewater [3]. Several removal methods have been developed, such as chemical deposition, ion exchange, and adsorption. A low concentration of Pb(II), can be separated with calix[4]arene-tetraacetate as adsorbents using the droplet-based microreactor system methods [4]. Sugarcane bagasse activated carbon (SCBA) is also effective in adsorbing Pb(II) [5]. Furthermore, Pb(II) absorption can be carried out using bisazocalix[4]arene [6], calix[4]resorcinarene derivatives [7], bentonite-decorated-calix[4]arene [8-10], modified beech sawdust [11], methoxyphenylcalix[4]resorcinarene [12], calixarene-grafted nanocomposites [13], polypyrrole-carbon composites [14], polyacrylamide [15], 5,11,17,23-tetra-(*t*-butyl)-25,26,27,28-tetrahydroxycalix[4]arene (TBCA) [16-18], poly-calix[4]arene [19]. The synthesis of

tribenzoyloxy-*p-tert*-butylcalix[4]arene can occur through two reaction routes, namely the formation of TBCA using *p-tert*-butylphenol with formaldehyde under alkaline conditions (NaOH) along with water smoke [20-23], as well as partial benzylation of *p-tert*-butylcalix[4]arene using benzoyl chloride in a mole ratio of 1:3.5 to yield 5,11,17,23-tetra-(*t*-butyl)-26,27,28-tribenzoyloxy-calix[4]arene (TBMTCA) [24]. Calixarene-based extractants for heavy metal ions removal from aqueous solutions have been reported [25]. Adsorption of methylene blue dye by calix[6]arene-modified has been reported [26]. Adsorption of Pb(II) and Cu(II) ions using bio-char [27], pulverized clay [28], chemically activated carbon [29], calix[6]arene-modified lead sulfide in paint (PbS), methylene blue dye [30], and cyclodextrin-calixarene [31]. The previously mentioned absorbents are relatively difficult in synthesis and expensive compared to TBCA and TBMTCA. Therefore, this paper reports the synthesis of TBCA and TBMTCA as Pb(II) adsorbents in an aqueous solution. Additionally, the kinetic and isotherm adsorption using several models are evaluated as well.

## ■ EXPERIMENTAL SECTION

### Materials

Synthesis of TBCA was conducted according to Busroni et al. [16] while the synthesis of TBMTCA was conducted according to Kim et al. [18]. Pb(II) stock solution, acetone, Na<sub>2</sub>SO<sub>4</sub> anhydrate, and K<sub>2</sub>CO<sub>3</sub> were purchased from Merck, and used without purification.

### Instrumentation

The instruments used in this study consist of laboratory glassware, heating and magnetic stirring analytical scales (Libror EB-30 Shimadzu), Buchii evaporators (R-124), melting point determinants (Electrothermal-9100), Fourier transform infrared spectrophotometry (FTIR, Shimadzu-8201PC), <sup>1</sup>H-NMR spectrometry (Agilent Variant NMR 400 MHz Proton Magnetic Spectrometry), atomic absorption spectrophotometry (AAS, Buck Scientific, Pb-AA-283.2-Lib3 lamps), and pH Meter (Janway 3505 pH Meter).

### Procedure

#### Synthesis of 5,11,17,23-tetra-(*t*-butyl)-26,27,28-tetrahydroxycalix[4]arene (TBCA)

The adsorbent of TBCA was synthesized using a procedure reported by Busroni et al. [16]. The crude product was crystallized from CHCl<sub>3</sub>-MeOH and dried to give white crystal powder with a yield of 46.07%; m.p. 340–343 °C. FTIR (KBr) 3410 cm<sup>-1</sup> (OH); 3055 cm<sup>-1</sup> (C<sub>sp2</sub>-H); 1620 and 1481 cm<sup>-1</sup> (C=C Ar); 2955 and 2870 cm<sup>-1</sup> (C<sub>sp3</sub>-H); 1481 cm<sup>-1</sup> (CH<sub>2</sub>); 1366 cm<sup>-1</sup> and (CH<sub>3</sub>). <sup>1</sup>H-NMR (400 MHz, DMSO-d<sub>6</sub>) can be identified by peaks at δ 7.1757 ppm for Ar-H, δ 4.3841 ppm for Ar-CH<sub>2</sub>-Ar proton H axial, δ 3.5124 ppm for Ar-CH<sub>2</sub>-Ar proton H equatorial, δ 10.3367 ppm for Ar-OH and δ 0.67; 3.09; 0.71 ppm for C(CH<sub>3</sub>)<sub>3</sub>. TBCA structure is shown in Fig. 1(a).

#### Synthesis of 5,11,17,23-tetra-(*t*-butyl)-26,27,28-tribenzoyloxy-calix[4]arene (TBMTCA)

The adsorbent of TBMTCA was synthesized according to the procedure reported by Kim et al. [18]. As much as 1.5 g (2.32 mmol) of the TBCA was added into dry CHCl<sub>3</sub> (30 mL) and pyridine (1.35 mmol). Afterward, the benzoyl chloride (0.95 mL; 8 mmol) was slowly added into dry CHCl<sub>3</sub> (30 mL). The mixture is stirred at room temperature for 3 h. The mixture is then washed and extracted with diethyl ether. Crude products are crystallized with CHCl<sub>3</sub>-MeOH and dried to give yellow-brown powder in 94.3% yield; m.p. 306–310 °C. FTIR (KBr) 3232 cm<sup>-1</sup> (-OH), 3054 cm<sup>-1</sup> (C<sub>sp2</sub>-H),

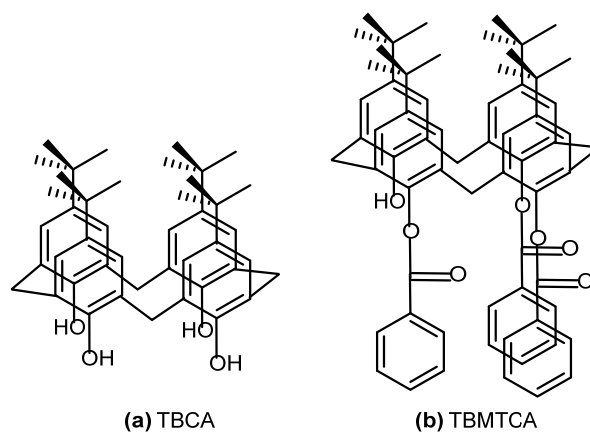


Fig 1. Structure of (a) TBCA, (b) TBMTCA

1605  $\text{cm}^{-1}$  (C=C aromatic), 1750  $\text{cm}^{-1}$  (C=O ester), 2870 and 2955  $\text{cm}^{-1}$  ( $\text{C}_{\text{sp}^3}\text{-H}$ ), 1458  $\text{cm}^{-1}$  ( $-\text{CH}_2-$ ), and 1204  $\text{cm}^{-1}$  (C-O ether).  $^1\text{H-NMR}$  (400 MHz,  $\text{DMSO-d}_6$ ): Partial benzylation can be identified by peaks at  $\delta$  7.0–8.2 ppm (m, 15H,  $\text{PhC=O}$ ) and  $\delta$  10.3370 ppm (s, 1H,  $\text{Ar-OH}$ ). Other proton peaks include two doublets at  $\delta$  4.37–4.35 and 3.51–3.48 ppm corresponding to Axial H. Increase in low single ethylene at  $\delta$  1.25 ppm from the proton group  $\text{C}(\text{CH}_3)_3$ . The aromatic protons are found at equatorial methylene at  $\delta$  7.0–8.2 ppm ( $\delta$  7.04 ppm (m, 4H phenyl,  $J = 7-10$  Hz),  $\delta$  7.17 ppm (s, 8H Ar-H),  $\delta$  7.33 ppm (t, 2H phenyl,  $J = 7-10$  Hz),  $\delta$  7.47 ppm (t, 4H phenyl,  $J = 7-10$  Hz),  $\delta$  7.60 ppm (t, 2H phenyl,  $J = 7-10$  Hz),  $\delta$  8.10 ppm (d, 3H phenyl,  $J = 7-10$  Hz). TBMTCA structure is shown in Fig. 1(b).

### Effect of pH on Pb(II) adsorption

Pb(II) solution 8 ppm (10 mL) with a variation pH of 3, 4, 5, and 6 was prepared. They were then added with 5 mg adsorbent and stirred for 180 min. The filtrate was analyzed with AAS.

### Effect of exposure time

The Pb(II) solution 8 ppm (10 mL) at pH 5 was added by 10 mg adsorbent and then stirred with a time variation of 10, 20, 30, 90, 180, and 240 min. It was then filtered and analyzed with AAS.

### Effect of initial Pb(II) concentration

The Pb(II) solution (10 mL) was prepared at pH 5 with various concentrations of 8, 16, 20, 24, and 30 ppm. The adsorbent (10 mg) was added and then stirred at the optimal exposure time. It was then filtered, and the filtrate was determined using AAS.

## RESULTS AND DISCUSSION

### Effect of pH

The effect of pH on the adsorption of Pb(II) was determined by observing the adsorption in various pH to reach the equilibrium point at a certain contact time until the adsorbent became saturated. The investigation results for the effect of pH on the adsorption of Pb(II) on the adsorbents are shown in Fig. 2.

At low pH values or acidic conditions, the solution contains large amounts of proton ions, leading to the

protonation of the hydroxyl groups on TBCA and TBMTCA adsorbents. The carbonyl group on TBMTCA actively binds metal ions. Protonated adsorbent species have low electron densities, thereby reducing the ability to bind Pb(II) cations and even culminating in a repulsion effect. Increasing the pH value to a certain point can improve the adsorption of metal ions because it reduces the inactivation of active groups with protons. The effect can be achieved by varying the initial pH of the Pb(II) cation solution in the pH range of 3–6. Other parameters, such as concentration and time, are kept constant. The pH of the solution strongly influenced the ability of adsorbents in adsorbing Pb(II) cations. In this case, the hydroxyl groups are weak Brønsted-Lowry acid with a  $\text{pK}_a$  for the first deprotonation of 4.11 [20]. It can also act as a Lewis base due to the presence of free electrons donated to Pb(II) ion as a Lewis acid. In other words, at  $\text{pH} < \text{pK}_a$ , the one hydroxyl group in the adsorbent can be protonated to produce a positively charged adsorbent surface [8]. The Pb(II) cations adsorption process will decrease because both have a positive charge. Conversely, when  $\text{pH} > \text{pK}_a$ , one or more hydroxyl groups can be deprotonated to produce a negatively charged adsorbent surface, which increases the interaction with positively charged cations. At low pH or acidic atmospheres, the solution contains large amounts of protons, culminating in the protonation of the hydroxyl and carbonyl groups that actively bind Pb(II) cations [20-23]. This protonated adsorbent species has a low electron density, thereby reducing the binding ability. The positive charge on the protonated groups might also cause a repulsion effect with the cations,

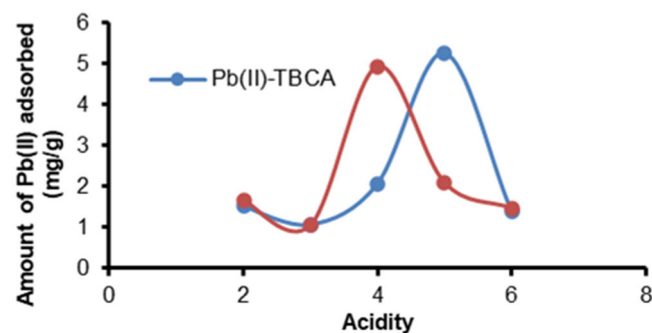


Fig 2. Effect of acidity on the adsorption of Pb(II)-TBCA, and Pb(II)-TBMTCA cations

which potentially reduces the absorption capacity. Increasing the pH value to a certain point can improve the Pb(II) adsorption because it reduces the inactivation of the active group by the protons, but at higher pH, most cations are hydrolyzed and clumped. This is due to the formation of various hydroxide complexes, including  $\text{PbOH}^+/\text{Pb}(\text{OH})_2/\text{Pb}(\text{OH})_3^-$  [2].

### Effect of Exposure Time and Initial Concentration toward Pb(II) Adsorption on TBCA and TBMTCA

The effect of exposure time on the adsorption of Pb(II) cations on TBCA and TBMTCA was determined by observing the time required to reach the equilibrium point. The exposure time between the ionic solution and the adsorbent ranges from 0 to 240 min. Based on the observations, the optimum exposure time for Pb(II) adsorption was 90 min on TBCA and TBMTCA (Fig. 3). Meanwhile, the optimum time is 30 min, with the number of Pb(II) cations adsorbed was 13.60 and 10.21 mg/g by both adsorbents, respectively.

Fig. 3 shows an increase in the number of ions adsorbed in the early minutes (10–30 min). This occurred because the active hydroxyl (OH) group on the TBCA surface had not interacted with the metal ions before the optimal time of 30 min. The functional group on the surface was saturated, and the change in the number of metal cations absorbed was no longer significant. It also occurred in the absorbance of Pb(II) cations at TBMTCA with an optimum time of 90 min. The investigation into the effect of variations in the concentration of Pb(II) cations into adsorbed metal cations in Fig. 3, seen at a low concentration of 8 ppm, then the concentration of metal adsorbed is also small because of the number of Pb(II) cations. Then the absorption of the number of metal cations will increase

according to the increase in Pb(II) cations in Fig. 3.

### Kinetics of Pb(II) Adsorption on TBCA and TBMTCA

The adsorption kinetics of Pb(II) was studied based on the kinetic formulation proposed by Lagergren and Ho models. The approach used was to calculate the change in time required for the adsorption process. In Lagergren kinetic formulation [27], adsorption is a pseudo-first order reaction that follows Eq. (1).

$$(q_e - q_t) = \log(q_e) - \frac{k_1}{2.303} t \quad (1)$$

where  $q_e$  is the total mass of metal adsorbed (mg/g),  $q_t$  is the mass of metal adsorbed at time  $t$  (mg/g), and  $k_1$  is the pseudo-first order Lagergren rate constant ( $\text{min}^{-1}$ ).

The adsorption kinetics can be also determined as a pseudo-second order reaction, which is often known as Ho's kinetic Eq. (2). In this equation, it is assumed that the adsorption kinetics follows the second order mechanism model, which means that the rate of adsorption (Fig. 4) is the square of the adsorbate concentration. The pseudo-second order equation (2) showing Ho is as follows Eq. (2).

$$\frac{t}{q_t} = \frac{1}{k_2 q_e^2} + \frac{1}{q_e} t \quad (2)$$

where  $k_2$  is a pseudo-second order rate constant ( $\text{g mg}^{-1} \text{min}^{-1}$ ).

The Lagergren kinetic model has a value of  $R^2$  almost equal to 1 the Ho-McKay as shown in Fig. 5 when  $R^2$  Ho is greater than  $R^2$  Lagergren. The curve with the linearity of the Lagergren kinetics model is higher than the Ho-McKay [25-26] with the Pb(II) cation. The adsorption rate constant of  $6.91 \times 10^{-3} \text{ min}^{-1}$  was determined through Lagergren's kinetic model using an oblique approach, as presented in Table 1.

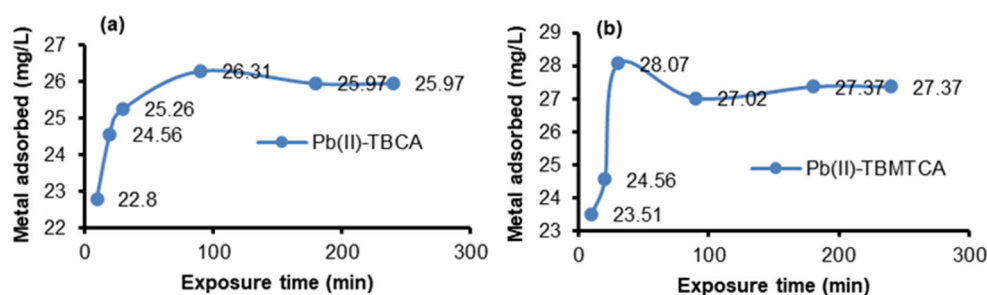


Fig 3. Effect of exposure time on the Pb(II) adsorption with (a) TBCA and (b) TBMTCA

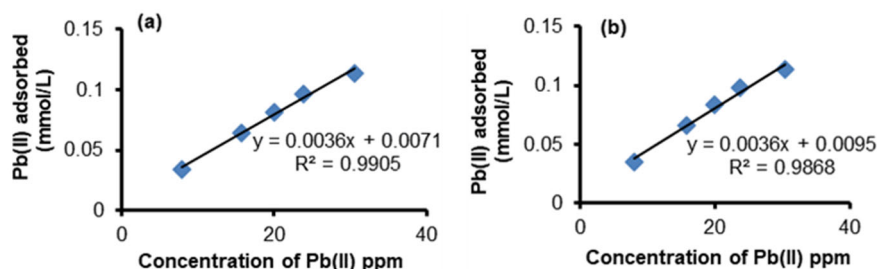


Fig 4. Effect of initial concentrations of Pb(II) cations on (a) TBCA and (b) TBMTCA

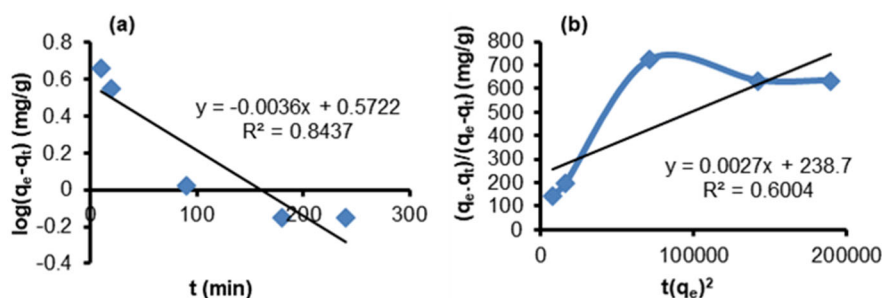


Fig 5. (a) Lagergren model (pseudo-first order kinetic,  $R^2 = 0.8437$ ) for Pb(II) adsorption on the TBMTCA; (b) Ho models (pseudo-second order kinetic,  $R^2 = 0.6004$ ) for Pb(II) adsorption on the TBMTCA

Table 1. Kinetic parameters of Pb(II) cations adsorption into TBCA and TBMTCA

Adsorbent	Kinetic Models*	Pb(II) cations	
		$R^2$	k
TBCA	Lagergren	0.836	$9.21 \times 10^{-3} \text{ min}^{-1}$
	Ho-McKay	0.957	$1.43 \times 10^{-1} \text{ g mg}^{-1} \text{ min}^{-1}$
TBMTCA	Lagergren	0.843	$6.91 \times 10^{-3} \text{ min}^{-1}$
	Ho-McKay	0.673	$0.03 \times 10^{-1} \text{ g mg}^{-1} \text{ min}^{-1}$

The bonding in Pb(II)-TBCA [16] and Pb(II)-TBMTCA material is an adsorbent and an excellent host for Pb(II) cations. The adsorption into TBMTCA trending kinetics Lagergren models was observed with constant values adsorption rate of  $6.91 \times 10^{-3} \text{ min}^{-1}$ . Furthermore, the observation results showed that the adsorption for the Pb(II) cation tends to follow the Langmuir isotherm. The optimum adsorption capacities in TBCA and TBMTCA were 137.29 and 128.46 mg/g, with adsorption energy of 6.51 and 5.81 kJ/mol, respectively. This is in line with a previous assumption, which stated that the interaction of Pb(II) cations with the TBMTCA and TBCA [16] compounds can be viewed as a chemical adsorption process. The TBMTCA compound has active sites in hydroxyl (-OH) and ester groups (-COOPh) that interact with the Pb(II) cation. In contrast, TBCA compounds have activities in the form of hydroxyl groups and a few

combinations, which means that the adsorption process only occurs chemically. Table 1 shows that the maximum adsorption capacity follows the HSAB concept stating that Pb(II) cation is an intermediate acid. According to this concept, a weak acid will bind to a weak base, while a strong acid will bind to a strong base. The active ester site on the adsorbent is the -COOPh group, a strong base, which is more stable interacting with metal cations, namely strong acids. The Pb(II) cation is the acid in the compound TBMTCA or strong base, but the bond is less stable, while -OH in TBCA is a weak acid or intermediate base, making the bond more stable.

Experimental data on the effect of contact time in Pb(II) cation adsorption with TBCA and TBMTCA were used and further analyzed to find the kinetics model, which includes the Lagergren (pseudo-first order) and the Ho-McKay (pseudo-second order). Furthermore,

the available data were processed and plotted into a straight-line equation to find a suitable model. The kinetic model with a correlation coefficient close to 1 is the most appropriate to explain the adsorption mechanism. The correlation coefficient ( $R^2$ ) comes from linear regression between  $\log(q_e - q_t)$  versus  $t$  (Lagergren kinetic model) and  $t/q$  versus  $t$  (Ho-McKay kinetic model), while  $q_e$  (mmol  $g^{-1}$ ) is the concentration of early metal ions. The figure shows the value of the adsorption rate constant using the slope or interception of the corresponding kinetic model equation (pseudo-second order).

The data analysis results of Pb(II) cations on TBCA in Fig. 6 show that the most suitable adsorption kinetics model was the Lagergren ( $R^2 = 0.8437$ ) with an absorption rate constant of  $9.21 \times 10^{-3} \text{ min}^{-1}$  compared to the Ho-McKay ( $R^2 = 0.6064$ ) with  $143 \times 10^{-3} \text{ g mg}^{-1} \text{ min}^{-1}$ . In the system with TBMTCA, which is the most suitable adsorbent, the adsorption of Pb(II) cations tended to have a higher correlation with the Lagergren kinetic model with an absorption rate constant of  $6.91 \times 10^{-3} \text{ min}^{-1}$  rather than Ho-McKay with  $143 \times 10^{-3} \text{ g mg}^{-1} \text{ min}^{-1}$ . The equations and the two systems' adsorption kinetics data are shown in Figs. 6 and 7.

### Adsorption Isotherm of Pb(II) on TBCA and TBMTCA

The Freundlich adsorption isotherm is obtained when a heterogeneous surface with non-uniform distribution of the adsorption heat over the surface. Meanwhile, in the Langmuir model, the assumption is that the absorption occurs at a specific homogeneous site in adsorbent. The mathematical equation of the Langmuir adsorption isotherm is:

$$\frac{C_e}{q_e} = \frac{1}{K \cdot X_m} + \frac{C_e}{X_m} \quad (3)$$

where  $K$  is the adsorption equilibrium coefficient (L/mol),  $X_m$  is the value of adsorption capacity (mol/L),  $C_e$  is the concentration of adsorbate in equilibrium (mol/L), and  $q_e$  is the amount of adsorbate absorbed in mol/g.

The mathematical equations of the Freundlich are as follows:

$$\log(q_e) = \log k + (n) \log C_e \quad (4)$$

where  $q_e$  is the number of grams adsorbed per adsorbent,  $C_e$  is the concentration at equilibrium, and  $k$  and  $n$  are constants.

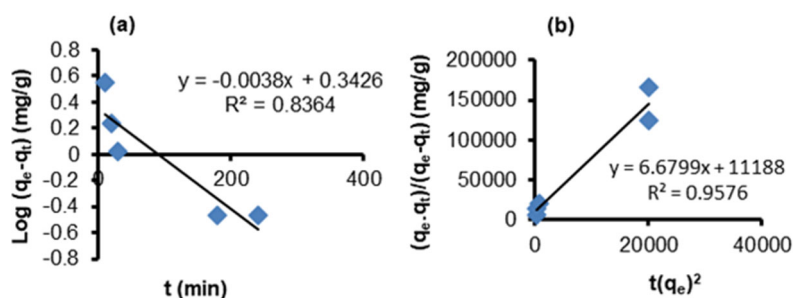


Fig 6. The kinetics of Pb(II) adsorption based on TBCA into (a) Lagergren and (b) Ho-McKay

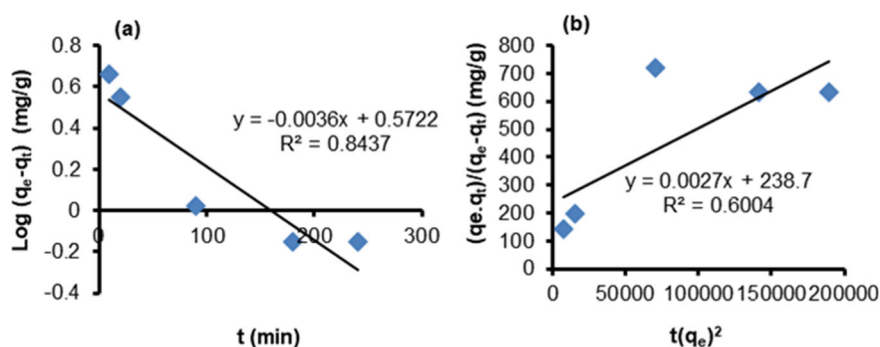


Fig 7. The kinetics of Pb(II) adsorption on TBMTCA, based on (a) Lagergren and (b) Ho-McKay models

The adsorption isotherm can be explained based on data obtained from the Pb(II) cations values at variations in the initial concentrations, as shown in Figs. 8 and 9 for Langmuir and Freundlich isotherm models, respectively.

The adsorption isotherm was determined using data on the concentration of metal cations adsorbed at equilibrium points. The isotherms were analyzed with the Langmuir isothermal models with  $(C_e/q_e = 1/(K.X_m) + C_e/X_m)$  and Freundlich ( $\log q_e = \log K + 1/n.\log C_e$ ), where  $q_e$  is the number of metal cations adsorbed at equilibrium (mmol/g),  $C_e$  is the concentration of metal cations in solution at equilibrium (mmol/L),  $X_m$  is the maximum adsorption capacity (mg/g), and  $K$  is the adsorption constant as shown in Figs. 8 and 9.

The adsorption isotherm analysis of Pb(II) cation in TBCA (Fig. 8) showed that the pattern of the two metal ions was more in line with the Langmuir isotherm adsorption model with  $R^2 = 0.971$  than Freundlich ( $R^2 = 0.628$ ). These results indicate that Pb(II) cations adsorbed on TBCA tend to form a monolayer on the surface. It was also assumed that maximum adsorption occurs when the interaction between all active groups, specific hydroxyl on TBCA and Pb(II) cations, forms a single layer with adsorption energy for each cation of 5.81 kJ/mol. The cation's adsorption is higher in the Langmuir isotherm

model ( $R^2 = 0.982$ ); hence, the mechanism and energy of 6.51 kJ mol<sup>-1</sup>, were similar for each cation. The parameters were obtainable from observations of both isotherms present in TBMTCA (Fig. 9). This shows that the adsorption pattern of Pb(II) cations refers to the Langmuir isotherm adsorption models which occur in one layer (monolayer). Furthermore, it is assumed that the maximum adsorption occurs in all active sites of OH and C=O groups. The adsorption energy between Pb(II) cations was 6.51 kJ/mol (Table 2). The maximum adsorption capacity can be explained based on the HSAB concept, which states that Pb(II) cations are hard medium acids and have a slight radius value. In this concept, intermediate acids interact with weak acids, while strong acids interact with complex bases [20-23]. The active site in the adsorbent is the OH group, and the C=O group is a strong base; hence, both groups will be less stable interacting with the Pb(II) cations, which is an intermediate acid group. The parameters of both isothermic observations are presented in Table 2. The adsorption pattern of Pb(II) cation refers to the Langmuir isotherm adsorption models, which occur in one layer (monolayer). It is assumed that the maximum adsorption occurs in all active sites, including OH and C=O groups. From Table 2, the optimum exposure time

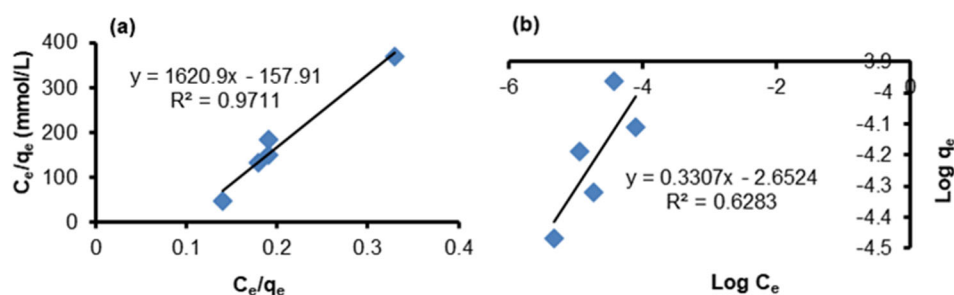


Fig 8. The adsorption isotherm of Pb(II) on TBCA based on (a) Langmuir and (b) Freundlich models

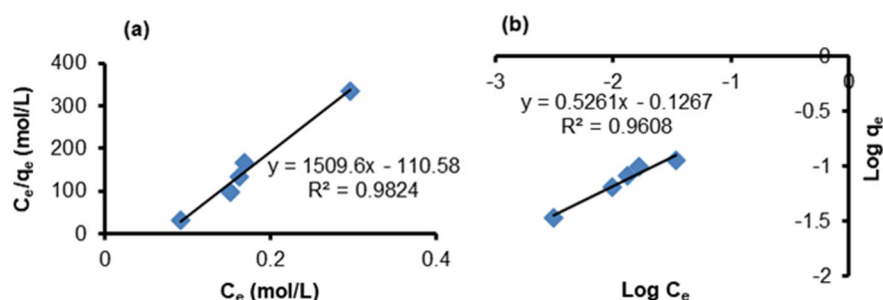


Fig 9. The adsorption isotherm of Pb(II) on TBMTCA based on (a) Langmuir and (b) Freundlich models

**Table 2.** Parameters of Langmuir and Freundlich isotherm models

Adsorbent	Metal	Langmuir			Freundlich			
		$X_m$ (mg g <sup>-1</sup> )	K (L mol <sup>-1</sup> )	$E_{ads}$ (kJ mol <sup>-1</sup> )	$R^2$	n	k	$R^2$
TBCA	Pb(II)	137.29	13.60	6.51	0.97	0.33	0.002	0.63
TBMTCA	Pb(II)	128.46	10.21	5.81	0.98	0.43	0.01	0.69

**Table 3.** Comparison of Pb(II) adsorption properties using different adsorbents

Adsorption study		Comparison studies of isotherm and kinetic					Ref.
Adsorbent	pH	Contact time (min)	Isotherm adsorption	Kinetic models	Adsorption capacity (mg/g)		
Pb(II)-TBCA	6.0	10	Intra-particle diffusion	Ho-McKay	-	[17]	
Pb(II)-Poly-Calixarene	4.0	180	Freundlich	Ho-McKay	187.63	[19]	
Pb(II)-TBCA	5.0	30	Langmuir	Ho-McKay	137.29	[16]	
Pb(II)-TBMTCA	4.0	90	Langmuir	Lagergren	128.46	[16]	

of Pb(II) cations was 30 min, and the amount of Pb(II) cations adsorbed by TBCA and TBMTCA was 137.29 and 128.46 mg/g, respectively. The desorption kinetics rate can be determined based on the time of interaction to reach the equilibrium state. General indicators for predicting adsorption are the reaction rate (k) and the correlation coefficient ( $R^2$ ). The adsorption isotherm parameters data of Pb(II) cations in TBCA and TBMTCA are briefly compared for adsorption studies presented in Table 3.

## ■ CONCLUSION

Based on the results, the Pb(II) adsorption on TBCA and TBMTCA follows the Ho-McKay kinetic model. TBMTCA is consistent with the Ho-McKay and the Lagergren kinetic models, while the adsorption isotherm model shows that the adsorption for Pb(II) on TBCA and TBMTCA materials is consistent both with Langmuir isotherms models. The maximum adsorption capacity for Pb(II) on TBCA and TBMTCA are 137.29 and 128.46 mg/g, respectively. Adsorption energy for the interaction of Pb(II)-TBCA, and Pb(II)-TBMTCA is 6.51 and 5.81 kJ/mol, respectively. The adsorption capabilities indicate good prospects in the removal of heavy metal cations from polluted water for environmental protection.

## ■ ACKNOWLEDGMENTS

The authors gratefully acknowledge the financial assistance provided by *Sumber Daya IPTEK dan DIKTI*

Project (Contract Number T/125/D2.3/KK.04.03/2019).

## ■ REFERENCES

- [1] Arifin, Z., Puspitasari, R., and Miazaki, N., 2012, Heavy metal contaminations in Indonesian coastal marine ecosystems: A historical perspective, *Coastal Mar. Sci.*, 35 (1), 227–233.
- [2] Hoang V.A., Nashihama, S., and Yoshizuka, K., 2021, Selective adsorption of lead(II) from aqueous, *Environ. Technol.*, 43 (14), 2124–2134.
- [3] Flora, G., Gupta, D., and Tiwari, A., 2012, Toxicity of lead: A review with recent updates, *Interdiscip. Toxicol.*, 5 (2), 47–58.
- [4] Kurniawan, Y.S., Ryu, M., Sathuluri, R.R., Iwasaki, W., Morisada, S., Kawakita, H., Ohto, K., Maeki, M., Miyasaki, M., and Jumina, J., 2019, Separation of Pb(II) ion with tetraacetic acid derivative of calix[4]arene by using droplet-based microreactor system, *Indones. J. Chem.*, 19 (2), 368–375.
- [5] Salihi, I.U., Kutty, S.R.M., and Isa, M.H., 2017, Adsorption of lead ions onto activated carbon derived from sugarcane bagasse, *IOP Conf. Ser.: Mater. Sci. Eng.*, 201, 012034.
- [6] Elçin, S., Karakuş, O.O., Kara, İ., and Deligöz, H., 2015, Synthesis and structural characterization of bisazocalix[4]arene with melamine: Metal ion extraction studies, *J. Mol. Liq.*, 202, 134–140.
- [7] Utomo, S.B., Jumina, J., Siswanta, D., and Mustofa, M., 2012, Kinetic and equilibrium model of Pb(II)



- and Cd(II) adsorption tetrakis-thiomethyl-C-methoxyphenylcalix[4]resorcinarene, *Indones. J. Chem.*, 12 (1), 49–56.
- [8] Jlassi, K., Abidi, R., Benna, M., Chehimi, M.M., Kasak, P., and Krupa, I., 2018, Bentonite-decorated calix[4]arene: A new, promising hybrid material for heavy-metal removal, *Appl. Clay Sci.*, 161, 15–22.
- [9] Chen, X., 2015, Modeling of experimental adsorption isotherm data, *Information*, 6 (1), 14–22.
- [10] Sugita, P., Purwaningsih, H., and Fathurrahman, M., 2015, Adsorption studies of Fe(III) ion on glutaraldehyde cross-linked chitosan and its application in purifying vetiver oil, *Int. J. Chem. Sci.*, 13 (4), 1805–1817.
- [11] Tashauoei, H.R., Hashemi, S., Ardani, R., Yavari, Z., and Asadi-Ghahhari, M., 2016, Adsorption of lead from aqueous solution by modified beech sawdust, *J. Saf. Environ. Health Res.*, 1 (1), 11–16.
- [12] Kesuma, E.P., Jumina, J., Ohto, K., and Siswanta, D., 2016, Synthesis of C-4-allyloxy-3-methoxyphenylcalix[4]resorcinarene from vanillin and its application as adsorbent of Pb(II) metal cation, *Orient. J. Chem.*, 32 (2), 769–775.
- [13] Kamboh, M.A., Wan Ibrahim, W.A., Rashidi Nodeh, H., Zardani, L.A., and Sanagi, M.M., 2018, Fabrication of calixarene-grafted magnetic nanocomposite for the effective removal of lead(II) from aqueous solution, *Environ. Technol.*, 40 (19), 2482–2493.
- [14] Alghamdi, A.A., Al-Odayni, A.B., Saeed, W.S., Al-Kahtani, A., Alharthi, F.A., and Aouak, T., 2019, Efficient adsorption of lead(II) from aqueous phase solutions using polypyrrole-based activated carbon, *Materials*, 12 (12), 2020.
- [15] Gu, S., Wang, L., Mao, X., Yang, L., and Wang, C., 2018, Selective adsorption of Pb(II) from aqueous solution by triethylenetetramine-grafted polyacrylamide/vermiculite, *Materials*, 11 (4), 514.
- [16] Busroni, B., Siswanta, D., Santosa, S.J., and Jumina, J., 2017, Study of Pb(II) and Fe(III) metal cations adsorption into *p-tert-butylcalix[4]arene* as adsorbent: Kinetic adsorption, *Int. J. Adv. Res.*, 5 (9), 574–580.
- [17] Moradi, O., Zare, K., Zekri, A.R., and Fakhri, A., 2012, Experimental modeling of the adsorption kinetics of Cd(II) and Pb(II) ions by calix[4]arene surface, *J. Phys. Theor. Chem.*, 9 (2), 67–76.
- [18] Kim, J.M., Chun, J.C., and Nam, K.C., 1997, Selective acyl and alkylation of monobenzoyl-*p-tert-butylcalix[4]arene*, *Bull. Korean Chem. Soc.*, 18 (4), 409–415.
- [19] Handayani, D.S., Jumina, J., Siswanta, D., and Mustofa, M., 2012, Adsorpsi ion logam Pb(II), Cd(II) dan Cr(III) oleh poli-5-allil-kaliks[4]arena tetraester, *JML*, 19 (3), 218–225.
- [20] Araki, K., Iwamoto, K., Shinkai, S., and Matsuda, T., 1990, "pK<sub>a</sub>" of Calixarenes and analogs in nonaqueous solvents, *Bull. Chem. Soc. Jpn.*, 63 (12), 3480–3485.
- [21] Pearson, R.G., 1963, Hard and soft acids and bases, *J. Am. Chem. Soc.*, 85 (22), 3533–3539.
- [22] LoPachin, R.M., Gavin, T., DeCaprio, A., and Barber, D.S., 2012, Application of the hard and soft, acid and bases (HSAB) theory to toxicant–target Interactions, *Chem. Res. Toxicol.*, 25 (2), 239–251.
- [23] Ho, Y.S., and McKay, G., 1999, Pseudo-second order model for sorption processes, *Process Biochem.*, 34 (5), 451–465.
- [24] Ho, Y.S., 2004, Citation review of Lagergren kinetic rate equation on adsorption reactions, *Scientometrics*, 59 (1), 171–177.
- [25] Konczyk, J., Nowik-Zajac, A., and Kozłowski, C.A., 2016, Calixarene-based extractants for heavy metal ions removal from aqueous solutions, *Sep. Sci. Technol.*, 51 (14), 2394–2410.
- [26] Rosly, N.Z., Abdullah, A.H., Kamarudin, M.A., Ashari, S.E., and Ahmad, S.A.A., 2021, Adsorption of methylene blue dye by calix[6]arene-modified lead sulphide (Pbs): Optimisation using response surface methodology, *Int. J. Environ. Res. Public Health*, 18 (2), 397.
- [27] Musumba, G., Nakiguli, C., Lubanga, C., Mukasa, P., and Ntambi, E., 2020, Adsorption of lead(II) and copper(II) ions from mono synthetic aqueous solutions using bio-char from *Ficus natalensis* fruits, *J. Encapsulation Adsorpt. Sci.*, 10, 71–84.
- [28] Priastomo, Y., Morisada, S., Kawakita, H., Ohto, K.,

- and Jumina, J., 2021, Improved precious metal adsorption by introduction of carboxylic acid groups on methylene crosslinked calix[4]arene resin matrix, *J. Inclusion Phenom. Macrocyclic Chem.*, 101 (1), 51–61.
- [29] Olaremu, A.G., 2021, Adsorption of lead from aqueous solution by pulverized local clay, *Scholar Int. J. Chem. Mater. Sci.*, 4 (5), 73–78.
- [30] Malise, L., Rutto, H., Seodigeng, T., Sibali, L., and Ndibewu, P., 2020, Adsorption of lead ions onto chemical activated carbon derived from waste tire pyrolysis Char: Equilibrium and kinetics studies, *Chem. Eng. Trans.*, 82, 421–426.
- [31] Cataldo, S., Lo Meo, P., Conte, P., Di Vincenzo, A., Milea, D., and Pettignano, A., 2021, Evaluation of adsorption ability of cyclodextrin-calixarene nanosponges towards  $Pb^{2+}$  ion in aqueous solution, *Carbohydr. Polym.*, 267, 118151.